 This article appeared in Silva, W. G. D. P.; Daudet, G.; Perez, S.; Thorwirth, S.; van Wijngaarden, J. *J. Chem. Phys.* 154, 164303 (2021) and may be found at https://doi-org.uml.idm.oclc.org/10.1063/5.0048699

Conformational preferences of diallylamine: A rotational spectroscopic and theoretical study

Weslley G. D. P. Silva,[1] Gabrielle Daudet,[1] Sem Perez,[1] Sven Thorwirth[2] and Jennifer van Wijngaarden[1*]

[1]Department of Chemistry, University of Manitoba, Winnipeg, Manitoba, R3T 2N2, Canada

[2]I. Physikalisches Institut, Universität zu Köln, Zülpicher Str. 77, 50937 Köln, Germany

*Corresponding author

Email: vanwijng@cc.umanitoba.ca

Phone: (204)474-8379

Fax: (204)474-7608

Abstract

The conformational space of diallylamine (DAA) was investigated using rotational spectroscopy from 7–19 GHz aided by quantum chemical calculations. Extensive conformational searches using density functional theory B3LYP-D3(BJ) and the *ab initio* MP2 method with the aug-cc-pVTZ basis set identified a total of 42 minima for DAA within ~22 kJ mol^{-1}. This reveals a strikingly rich conformational landscape for this secondary amine with two equivalent substituents. Experimentally, transitions belonging to four low energy conformers (I, II, III and IV) were unequivocally assigned in the rotational spectrum and their patterns were confirmed by the presence of the hyperfine structure owing to the ^{14}N quadrupolar nucleus. The relative intensities of the observed transitions suggest a conformational energy ordering of I < II < III < IV. Natural bond orbital and non-covalent interaction calculations reveal that the geometric preferences for the observed conformers are governed by an interplay of subtle attractive interactions (including hyperconjugation involving the lone pair at nitrogen) and repulsive effects.

Introduction

After the introduction of the term “conformation” by Barton in 1950,[1] chemists have increasingly treated molecules as flexible entities which vary in shape and function depending on their chemical environment. Correspondingly, the effects ruling the geometries of molecular systems with a broad range of applications from biological to astrochemical processes have garnered widespread interest. While the chemistry of amines and amino acids, the building blocks of proteins, have been widely studied in biological systems, their formation under astrophysical conditions is still an intriguing question.[2] The identification of routes for formation of biomolecules in space may lead to explanations as profound as the origins of life.[2,3] As highlighted by Melosso *et al*,[3] although several amines (e.g. aminoacetonitrile,[4] methylamine[5,6]) that are potential precursors of amino acids have been reported in the interstellar medium (ISM),[7] the detection of others remains elusive. Detailed spectroscopic studies of novel N-bearing molecules of astrochemical interest, or that may be used to generate transient candidates for future detection, are central to elucidating the chemistry of prebiotic species in the ISM.[2,3]

Recently, the rotational spectrum of allylmethylamine[8] (AMA) whose thermal decomposition leads to the formation of propylene[9] and methanimine[10] was reported. Apart from providing necessary information for radioastronomical detection, this study detailed the successful characterization of four low energy conformers below 4 kJ mol^{-1}. Diallylamine, DAA, is a natural, interesting extension of this study from both physical and chemical points of view. In comparison to the structure of AMA in which the amino group is bonded to allyl and methyl moieties, DAA possesses two equivalent allyl substituents

(Figure 1). While the presence of four dihedral angles may lead to additional conformations, there are potentially more competing interactions between the two allyl substituents and symmetry considerations at play. As a potential precursor to generate novel species in the laboratory, the thermal decomposition of DAA is known to favour by-products of astrochemical interest including 2-propene-1-imine.[11] Thus, complete rotational spectroscopic characterization of DAA lays essential groundwork for future studies of novel species that are candidates for astronomical searches. So far, the pure rotational spectrum of DAA has not been investigated.

In this work, the conformational preferences of DAA are explored through interpretation of its rotational spectrum collected using Fourier Transform Microwave (FTMW) spectroscopy and aided by density functional theory (DFT) and *ab initio* quantum chemistry calculations (MP2, CCSD(T)). The computational results indicate a rich and complex conformational landscape for DAA making it an excellent, but demanding, prototype to evaluate the performance of quantum chemical models in reproducing energetic and spectroscopic properties of highly flexible molecules. While no fewer than 17 conformers have been identified within 7 kJ mol^{-1} using quantum chemistry calculations, rotational transitions corresponding to four low energy conformers were assigned with added confirmation from analysis of the characteristic ^{14}N hyperfine patterns. Information about the relative energy ordering of the identified conformers, their interconversion barriers and spectroscopic signatures are rationalized here using high-level B3LYP-D3(BJ), MP2 and CCSD(T) calculations. Natural bond orbital[12] and non-covalent interaction[13] analyses were also carried out to map out the stereoelectronic effects ruling the observed conformational preferences.

Experimental methods

Rotational spectra of DAA were recorded using a chirped-pulse (cp) and a cavity-based Balle-Flygare (BF) FTMW spectrometer which have been reported in detail previously.[14,15] Briefly, a gas mixture containing ~1% of DAA (99.0% purity, Sigma Aldrich Canada; bp: 111–112 °C) in neon (~200 kPa) was prepared at room temperature and introduced into the spectrometers' high vacuum chambers through a pulsed nozzle (1 mm diameter orifice). The expansion of the gas mixture inside the chambers creates a supersonic jet in which the species are probed in a collision-free environment. Initially, a broadband spectrum was collected using the cp-FTMW spectrometer in the frequency range 8–18 GHz (segments of 1 GHz each) to serve as a survey spectrum from which the most intense rotational transitions of the different conformers were identified. Final frequency measurements of all accessible transitions were performed using the BF-FTMW instrument to resolve the hyperfine structure due to the presence of the ^{14}N quadrupolar nucleus and to record transitions at higher frequencies up to 19 GHz. Transitions collected using the cavity-based instrument appear as Doppler doublets and individual lines have widths of ~7 kHz (FWHM). The uncertainty in the measurement of the line positions is typically ±2 kHz.

Computational methods

The molecular geometry of DAA has four dihedral angles (α, β, γ, and θ, Figure 1) about which internal rotations can give rise to different conformers. For each torsional angle, three staggered conformations (one *trans* and two *gauche*) can exist whose combinations result in a total of 81 possible geometries for DAA. This comes from the prediction that the number of potential conformers in a molecule is 3^n where n= 4 is the number of dihedral angles. Initially, each of these 81 possible geometries were fully optimized using the DFT dispersion-corrected B3LYP[16] functional with Becke-Johnson (BJ) damping,[17,18] also known as B3LYP-D3(BJ), and the *ab initio* second-order Møller-Plesset (MP2)[19] perturbation theory method. For both sets of calculations, Dunning's aug-cc-pVTZ[20] basis set was used. Harmonic frequency calculations were carried out at the same levels of theory to verify the nature of the stationary points and to obtain the electronic energies with zero-point energy (ZPE) corrections. From the 81 initial geometries, the calculations yielded 42 true energy minima due to the presence of equivalent structures generated from the method above (e.g. mirror images). All preliminary optimization and frequency calculations were done using the Gaussian 16 software.[21] Given the rich conformational space of DAA and the close relative energies between the lowest-lying conformers from the preliminary calculations, we also employed the coupled-cluster singles and doubles (CCSD) theory augmented by a perturbative treatment of triple excitations, CCSD(T)[22] for the six most stable rotamers. Two approaches were considered for the coupled-cluster calculations including (1) single-point energy calculations at the CCSD(T)/aug-cc-pVTZ level using the MP2/aug-cc-pVTZ optimized geometries and (2) full optimization and harmonic frequency calculations at the

CCSD(T)/ANO0[23] level of theory. All CCSD(T) calculations were performed using CFOUR.[24,25] Finally, to investigate the stereoelectronic effects ruling the conformational preferences of DAA, non-covalent interaction (NCI)[13] and natural bond orbital (NBO)[12] analyses were performed using the NCIPLOT[26] and NBO7[27] programs, respectively.

Results

Conformational space of DAA

The quantum chemical calculations indicate an extremely rich conformational space for DAA in which a total of 42 unique conformers exist within ~22 kJ mol^{-1}. Since higher energy conformers are not expected to be populated at room temperature (see Table 1), only 17 minima whose energies are within 7 kJ mol^{-1} were considered further. The calculated energetic and spectroscopic parameters for these 17 conformers obtained using the B3LYP-D3(BJ) and MP2 methods are given in Table 1 while in Figure 1 we provide pictorial representations for the four low energy conformers which were experimentally detected (as presented in the spectral analysis section). The geometries corresponding to all 17 minima along with their Cartesian coordinates are given in the supporting information (SI) file in Figure S1 and Tables S1–S17, respectively. The conformers are labeled using Roman numerals from I–XVII based on their B3LYP-D3(BJ) relative energy ordering with conformer I possessing the most stable arrangement. Although the geometries of the conformers obtained at the B3LYP-D3(BJ) and MP2 levels are very similar, their relative energy orderings differ as seen in Table 1. The results from the higher *ab initio* CCSD(T) level (Table 1) also show a unique energy ordering but match

the predictions from B3LYP-D3(BJ) theory for the lowest two conformers. It is worth noting that since the six most stable conformers are almost isoenergetic (< 3 kJ mol^{-1}), the slight differences in their ranking are a direct consequence of this highly competitive equilibrium making it difficult to come up with a conclusive quantitative picture.

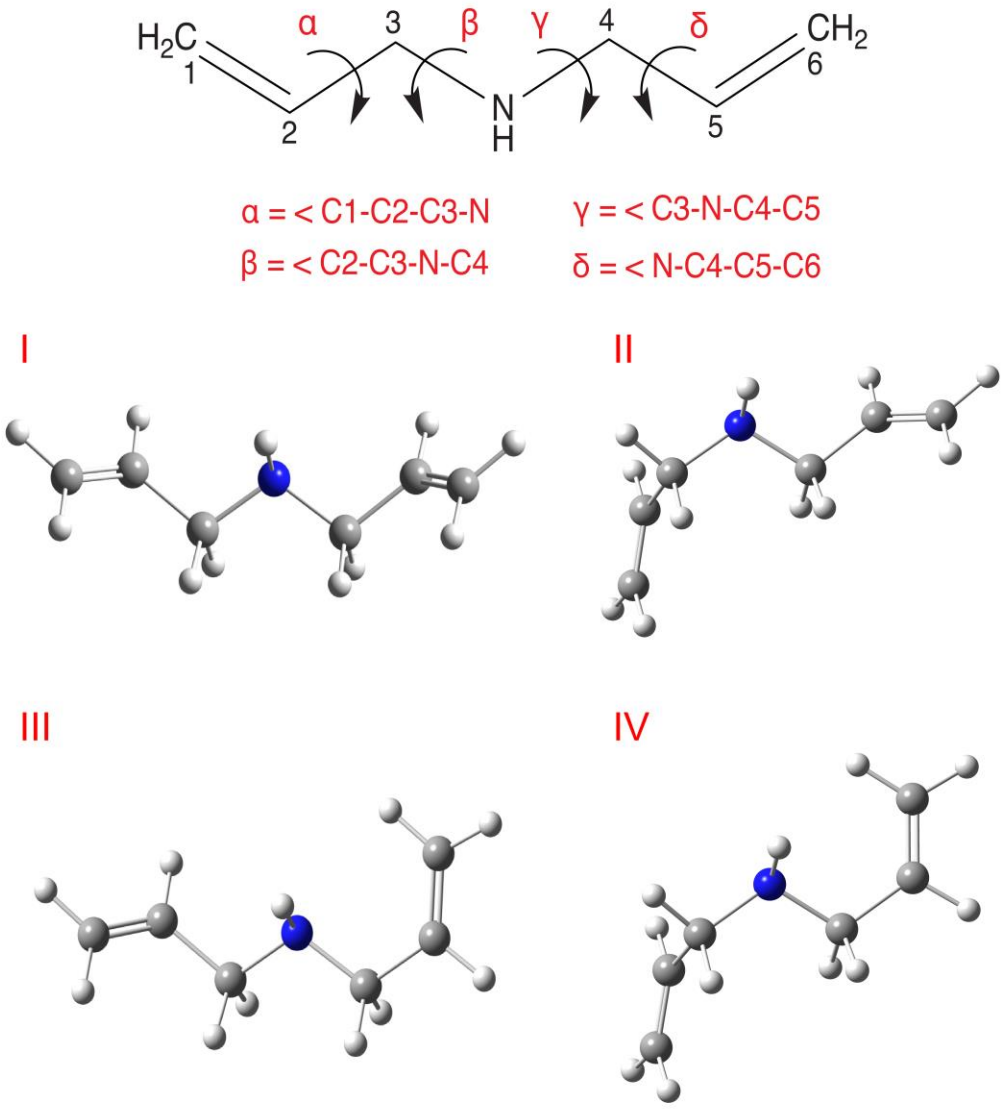

Figure 1. The four low energy conformers of DAA (bottom) studied experimentally, which arise due to internal rotations around the α, β, ɣ and δ dihedral angles (top). The angles for these and the other low energy conformers are summarized in Figure S1.

Table 1. Calculated energetic (relative energy with ZPE corrections ΔE_{ZPE} in kJ mol^{-1} and population P at 298K in %) as well as spectroscopic parameters (rotational constants A, B and C in MHz and electric dipole moment components μ_a, μ_b, μ_c in Debye) for the 17 most stable conformers of DAA within ~7 kJ mol^{-1}.

	B3LYP-D3(BJ)/aug-cc-pVTZ				MP2/aug-cc-pVTZ				CCSD(T) ANO0			CCSD(T) aug-cc-pVTZ[a]
Conformer	ΔE_{ZPE}	P_{298K}	$A/B/C$	$\lvert\mu_a\rvert/\lvert\mu_b\rvert/\lvert\mu_c\rvert$	ΔE_{ZPE}	P_{298K}	$A/B/C$	$\lvert\mu_a\rvert/\lvert\mu_b\rvert/\lvert\mu_c\rvert$	ΔE_{ZPE}	$A/B/C$	$\lvert\mu_a\rvert/\lvert\mu_b\rvert/\lvert\mu_c\rvert$	ΔE
I	0.0	17.6	10389/914/900	0.0/0.1/0.7	0.2	14.8	9703/936/916	0.0/0.3/0.8	0.0	9814/912/896	0.0/0.3/0.8	0.0
II	0.6	13.8	7346/1090/1024	0.0/0.3/0.8	0.0	16.0	7147/1119/1046	0.0/0.1/0.9	1.1	7142/1086/1018	0.0/0.2/0.9	0.5
III	1.5	9.6	8071/1045/967	0.2/0.7/0.6	2.0	7.1	7876/1063/984	0.2/0.7/0.8	1.9	7863/1039/963	0.2/0.6/0.8	1.4
IV	2.1	7.7	6842/1175/1108	0.2/0.1/1.0	1.8	7.7	6723/1206/1130	0.3/0.0/1.0	3.0	6677/1172/1104	0.2/0.0/1.0	1.9
V	2.1	7.5	3627/1837/1394	0.6/0.0/0.7	0.2	14.9	3522/1961/1448	0.6/0.2/0.8	2.1	3548/1832/1382	0.6/0.1/0.7	1.5
VI	2.3	6.9	5919/1185/1067	0.4/0.5/0.4	2.1	6.9	5663/1231/1099	0.4/0.7/0.5	1.8	5647/1192/1066	0.4/0.6/0.5	2.5
VII	2.8	5.7	5984/1266/1062	0.0/1.0/0.6	3.7	3.6	5966/1286/1076	0.0/1.0/0.7				
VIII	3.1	5.0	6736/1210/1098	0.2/1.1/0.4	2.8	5.3	6708/1235/1119	0.2/1.1/0.5				
IX	3.8	3.9	5279/1398/1276	0.1/1.2/0.3	3.5	3.9	5232/1437/1309	0.1/1.2/0.4				
X	3.9	3.6	7335/1178/1079	0.7/0.4/0.5	4.1	3.1	7110/1213/1104	0.8/0.5/0.6				
XI	4.1	3.4	5333/1346/1145	0.5/0.3/0.2	4.5	2.6	5054/1432/1194	0.5/0.6/0.3				
XII	4.1	3.3	7402/1054/985	0.3/0.6/0.2	5.0	2.1	6920/1094/1014	0.4/0.8/0.3				
XIII	4.1	3.3	4657/1451/1381	0.5/0.3/0.3	3.7	3.6	3830/2009/1783	0.6/0.7/0.1				
XIV	4.5	2.9	5631/1269/1157	0.3/0.1/0.7	4.4	2.7	5223/1363/1216	0.4/0.4/0.7				
XV	5.1	2.2	4554/1501/1413	0.9/0.2/0.8	4.0	3.2	4427/1577/1471	0.9/0.0/0.8				
XVI	5.5	1.9	12389/894/883	0.0/0.3/0.8	5.8	1.5	11992/906/896	0.1/0.3/0.9				
XVII	5.9	1.6	5878/1310/1219	0.7/0.3/0.3	6.7	1.1	5626/1368/1265	0.8/0.4/0.4				

[a]CCSD(T) single point calculation performed using the MP2/aug-cc-pVTZ structure.

Spectral analysis

Guided by the calculated rotational parameters for each conformer from Table 1, four sets of rotational transitions were assigned in the broadband spectrum (Figure 2A). The observed lines were mainly *b*- and *c*-type transitions consistent with the predicted patterns for conformers I, II, III and IV and exhibited partially resolved structure from the ^{14}N quadrupolar nucleus. The initial assignments were later confirmed using the cavity-based BF-FTMW instrument which features higher resolution and sensitivity allowing the hyperfine splittings to be better resolved. A sample of the BF-FTMW spectrum for conformer I is shown in Figure 2B. Based on careful intensity measurements of selected transitions and considering the calculated dipole components from Table 1, we estimate the relative population trend in the supersonic jet to follow the energy ordering I > II > III > IV. Despite further experimental efforts, no transitions belonging to other conformers of DAA could be assigned.

Transitions for each observed conformer were fitted with Pickett's SPFIT program[28] using Watson's S-reduced[29] Hamiltonian in the I^r representation to determine experimental rotational, quartic centrifugal distortion and ^{14}N quadrupole coupling constants. The resulting spectroscopic parameters are provided in Table 2 while the transition frequencies and fit residuals are given in Tables S18–S21. It is worth noting that while the fits for conformers II and IV showed satisfactory rms (root-mean-square) errors (below ~2 kHz) by fitting only the χ_{aa} and χ_{cc} diagonal elements of the ^{14}N nuclear quadrupole tensor, the position of some hyperfine components for conformers I and III were sensitive to the off-diagonal χ_{bc} element. For all four conformers, the determined

spectroscopic constants show good agreement with the computational predictions (Table S22).

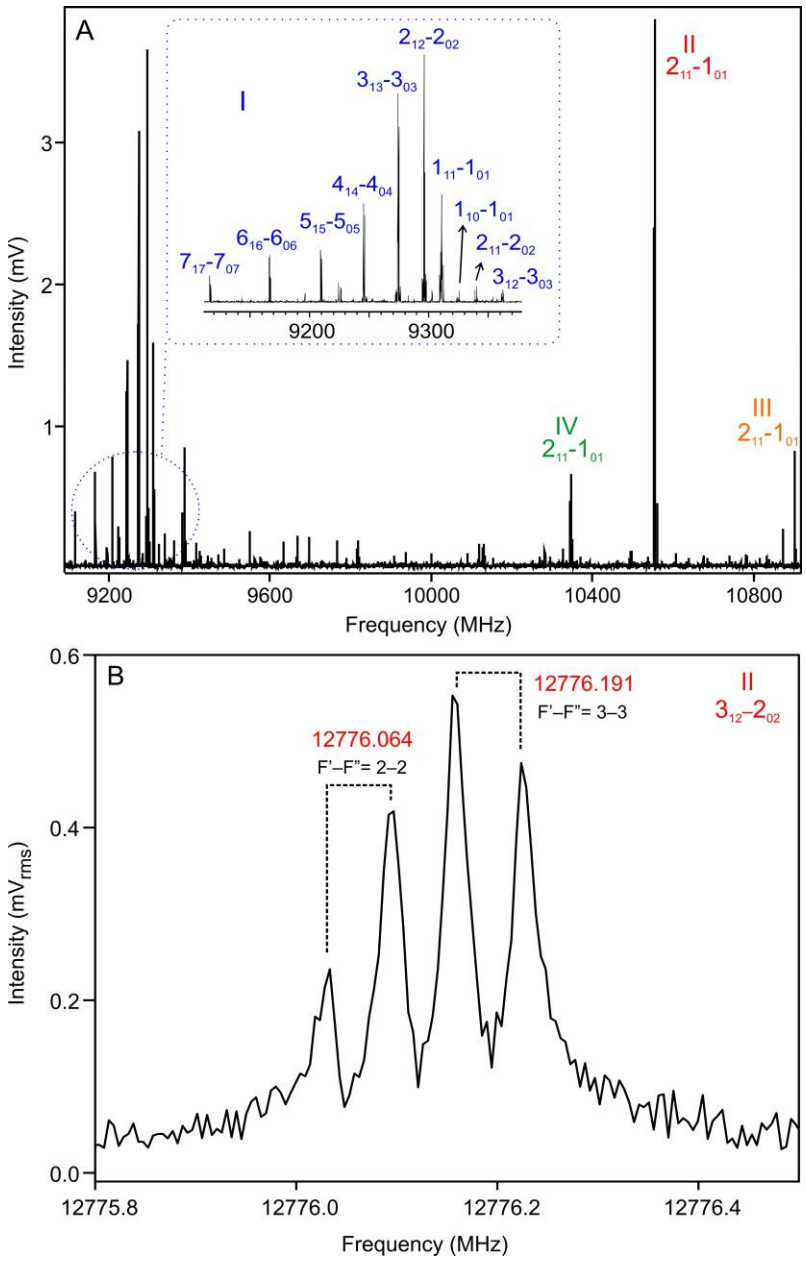

Figure 2. A) Sample of the cp-FTMW spectrum (1 million FIDs averaged) highlighting selected rotational transitions observed for conformers I, II, III and IV. B) BF-FTMW spectrum of the 3_{12}–2_{02} transition (340 cycles) of conformer II showing the F'–F" = 2–2 and F'–F" = 3–3 hyperfine components.

Table 2. Ground state spectroscopic parameters obtained for the four observed conformers of DAA.

	Conformer			
Parameter	I	II	III	IV
A (MHz)[a]	10227.44439(45)	7272.09620(64)	7993.5967(10)	6810.7226(20)
B (MHz)	916.42068(24)	1094.03684(17)	1047.19699(41)	1178.51168(56)
C (MHz)	901.86241(25)	1026.09596(18)	969.71266(35)	1110.72422(72)
D_J (kHz)[b]	0.1766(65)	0.2479(21)	0.1570(47)	0.321(20)
D_{JK} (kHz)	-13.787(29)	-4.3097(87)	[-4.602354214]	-8.69(17)
D_K (kHz)	[384.368818]	65.03(16)	[74.754307]	[93.229991]
d_1 (kHz)	-0.03376(39)	-0.04808(49)	-0.0198(22)	[-0.014171507]
d_2 (kHz)	[0.000566]	[-0.001099]	[0.0009053911]	[-0.00422286]
χ_{aa} (MHz) [c]	2.8865(19)	2.6706(12)	-0.0198(22)	2.6339(74)
χ_{cc} (MHz)	-4.1065(13)	-5.0108(12)	-3.1314(19)	-4.9781(63)
χ_{bc} (MHz)	-2.506(20)		3.09(23)	
σ (kHz)[d]	2.0	1.1	1.4	2.1
N[e]	71	49	29	12
$\mu_a/\mu_b/\mu_c$[f]	n/y/y	n/y/y	n/y/y	n/y/y

[a]Rotational constants; [b]quartic centrifugal distortion constants; [c]^{14}N nuclear quadrupole coupling constants; [d]root-mean-square of the fit; [e]number of lines in the fit; [f]electric dipole moment components ("y" if observed and "n" if not observed). Values in brackets [ ] were fixed to the values obtained at the B3LYP-D3(BJ)/aug-cc-pVTZ level of theory. A complete set of calculated constants for conformers I, II, III and IV is provided in Table S22.

Discussion

A surprisingly competitive conformational landscape is revealed for DAA by using a combination of FTMW spectroscopy and quantum chemistry calculations. Both DFT and *ab initio* methods suggest the existence of 17 conformers within ~7 kJ mol^{-1}. Four low energy conformers whose electronic energies with ZPE corrections are within 3 kJ mol^{-1} of the global minimum (by all methods employed) were unambiguously detected in the jet-cooled rotational spectrum. Although conformers V through XVII are predicted to have transitions in the range of our spectrometer, patterns consistent with their geometries were not identified despite careful searches. Conformers VII–XVII are expected to have relative populations smaller than 6% at 298K and coupled with their small calculated electric dipole moments (Table 1), their transitions will be less intense and may fall below the sensitivity of the spectrometers.

The lack of spectra features attributable to V and VI is more intriguing, however, as they are expected to be as populated as other detected conformers and possess similar electric dipole moment components (Table 1). In studies of molecules with multiple degrees of conformational flexibility, Godfrey and co-workers[30,31] suggest that MP2 calculations of the relative energies of conformers are only reliable to within roughly 2 kJ mol^{-1}. Thus, the populations of conformers V and VI of DAA could presumably be lower than predicted (Table 1) and, like conformers VII-XVII, their rotational transitions may fall below our detection limit. A second possibility is conformational relaxation to lower energy forms in the supersonic jet. Empirically, it has been shown for small molecules and complexes that interconversion barriers smaller than ~5 kJ mol^{-1} allow for efficient relaxation to lower energy forms in the molecular beam,[32] while for larger molecules with

multiple dihedral angles (as in DAA), higher barriers may be needed to prevent such interconversion.[30,31,33] Given the geometric similarities of conformers V and VI with II and I, respectively, we modeled possible interconversion pathways between conformers V→II and VI→I which largely requires changes in the ɣ dihedral angle. The results are given in Figure 3. The estimated barrier heights for the conformational cooling from V→II (~13.1 kJ mol^{-1}, 12.3 kJ mol^{-1} ZPE-corrected) and VI→I (~13.0 kJ mol^{-1}, 12.5 kJ mol^{-1} ZPE-corrected) are close to the 12 kJ mol^{-1} energy barrier separating the two lowest energy forms of β-alanine[33] where partial relaxation was reported. This suggests that conformers V and VI may also experience relaxation via the re-arrangements shown in Figure 3 or lower energy pathways requiring more concerted changes along multiple coordinates.

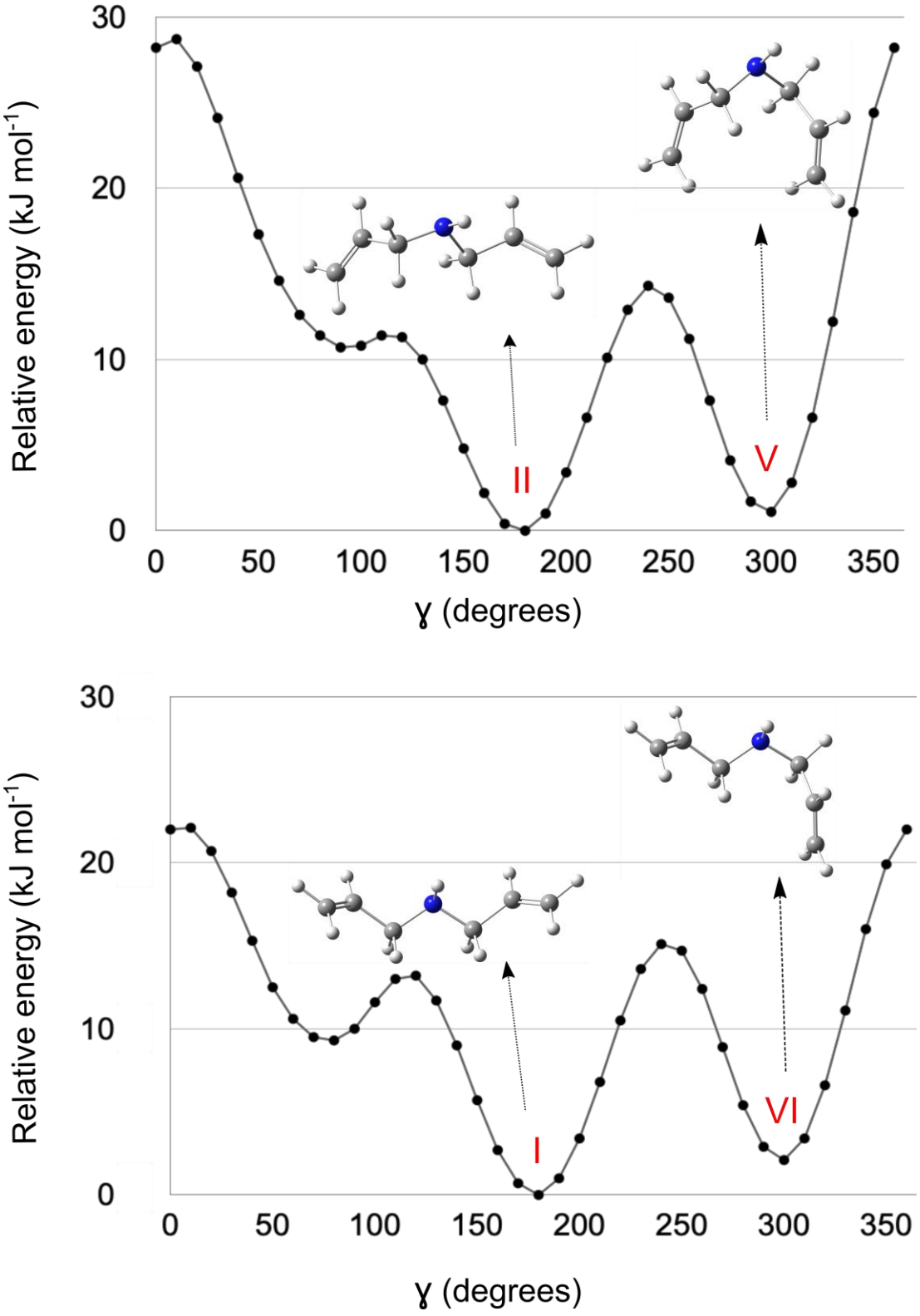

Figure 3. Relaxation pathways V→II (top) and VI→I (bottom) obtained at the B3LYP-D3(BJ)/aug-cc-pVTZ level of theory.

By inspecting the relative intensities of select transitions in our spectra, the experimental stability ordering (I > II > III > IV) matches the trend predicted by the B3LYP-D3(BJ), CCSD(T)/aug-cc-pVTZ//MP2 and, for the most part, the CCSD(T)/ANO0 calculations whereas the MP2 results suggest a different stability ranking of II > I ~ V > IV > III in which conformer II is the global minimum instead of I. This is not surprising as the energy difference between II and I is very small (~0.2–0.5 kJ mol^{-1}) at all levels of theory and hence these conformers should be treated as nearly isoenergetic. The inconsistencies in the results from the three computational methods is purely a consequence of the very small energy differences between the different conformers. Overall, the equilibrium rotational, quartic centrifugal distortion and ^{14}N quadrupole coupling constants from B3LYP-D3(BJ) provided the best match with the experimental ground state values for the conformers of DAA. This agrees with recent reports[34,35] for other conformer mixtures in which DFT-corrected functionals have shown good consistency with experimental data. B3LYP-D3(BJ), therefore, remains a powerful, affordable, widely accessible and accurate method to predict spectroscopic parameters of complex organic molecules.

To identify the underlying reasons for the highly competitive conformational space and dense rotational spectrum of DAA, we compared the results of DAA with those recently reported for the related diallyl disulfide (DADS)[36] compound. Although DADS is larger and contains more dihedral angles, only its non-symmetric C_1 global minimum geometry was observed in the rotational spectrum (in contrast to four conformers for DAA detected here). The dense spectrum of DAA is likely a consequence of both the relatively high energy barriers between conformers (which hinders their full relaxation into the

global minimum structure) and the additional conformational complexity introduced by the orientation of the hydrogen of the amino group. The global minimum of DADS is stabilized by a weak C–H···π hydrogen bond between the methylene subunit on one side of the S–S bridge with the π-electron cloud of the allyl group on the opposite side, while in conformer I of DAA, the amino hydrogen and both allyl groups point out of the plane of the C-N-C link in the same direction giving C_s-symmetry. These differences in the molecular structures of the most energetically favoured geometries of DADS (C_1) and DAA (C_s) highlight an unanticipated system-dependence and degree of diversity in the conformational landscape of allylic compounds.

Although the molecular structures for the most preferred conformers of DAA and DADS are surprisingly different, the lowest energy structure of AMA, with one allyl and one methyl substituent, is closely related to that of DAA. In the global minimum geometry of AMA,[8] the allyl and amino hydrogen also point out of the plane of the C-N-C bridge in the same direction. This was shown to simultaneously favour the formation of stabilizing orbital interactions involving the lone pair at nitrogen (n_N) and to minimize destabilizing effects from steric repulsion. To investigate whether the conformers of DAA are driven by analogous orbital interactions, we performed NCI and NBO calculations. The NCI analysis (Figure 4) reveals that attractive forces (blue-green regions) are found in the isosurfaces of conformers II (C–H···π), III (C–H···N) and IV (C–H···π and C–H···N) but not in conformer I. The C–H···π interactions across the C-N-C bridge in conformers II and IV resemble those responsible for the lowest energy conformation of DADS[36] but are not sufficient to explain the stability ordering of the conformers of DAA. The C–H···π and C–H···N interactions found in conformers II and III of DAA, respectively, have also been identified

in some of the low energy forms of AMA[8] having a similar orientation of the allyl group involved in the intramolecular contact. Both types of interactions are found in conformer IV of DAA, contributing to its low relative energy of ~3 kJ mol^{-1}, and arise from the two allyl moieties adopting orientations similar to those found in one side chain each of conformers II and III. It is worth noting that each of these attractions are accompanied by repulsive interactions (red regions) of similar magnitudes which are related to steric repulsion from formation of a five-membered ring once the intramolecular contact is established. Since conformer I does not show any such contacts, these interactions cannot be the only forces driving the conformational preferences of DAA.

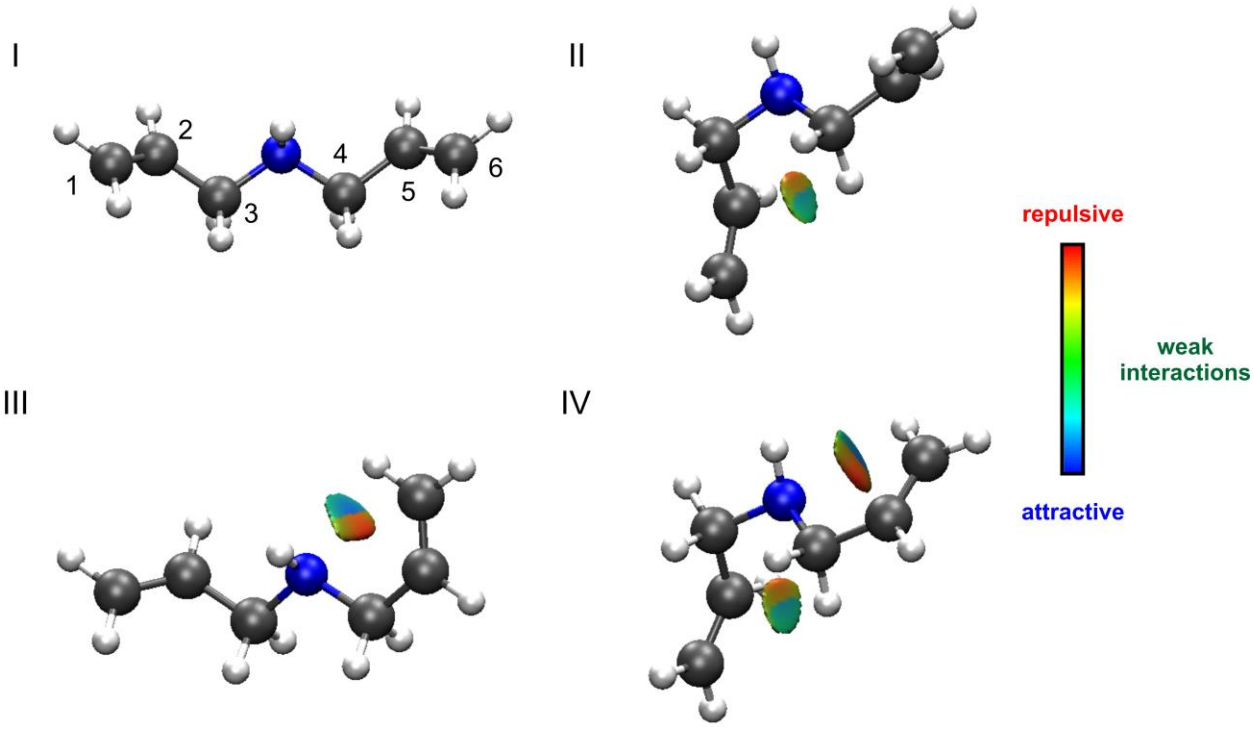

Figure 4. NCI isosurfaces (s= 0.06, colour scale of -0.02 < ρ < 0.02 au) for the four observed conformers of DAA.

To better understand the relative energy orderings and to verify the presence of orbital interactions in the conformers of DAA, we invoked NBO analysis to capture hyperconjugative effects involving occupied and empty orbitals. The NBO calculations reveal that charge transfer interactions from n_N to the antibonding orbitals of the C–H (methylene), C–C and C=C bonds of the allyl side chains play a role in the stabilization of the observed conformers of DAA. A summary of selected hyperconjugative interactions, obtained with the NBO analysis, and their corresponding second-order perturbation energies (E_2) is given in Table 3. The results show very similar interactions for the four conformers with the exception of the $n_N \rightarrow \pi^*_{C5–C6}$ which is only found in conformers I and II as the geometries allow for favourable orbital superposition of both allyl moieties with the amino group. In Figure S2, pictorial representations corresponding to the $n_N \rightarrow \pi^*_{C–C}$ interactions in I, II, III and IV are provided. Although the estimated E_2 values for certain interactions such as $n_N \rightarrow \sigma^*_{C2–C3}$ are different for the various conformers, none of these effects solely drive the conformational preferences. Based on the NCI and NBO calculations, we assert that a combination of subtle effects contributes to the highly competitive equilibrium of DAA. The high stability of conformer I is likely due to the arrangement of the two equivalent allyl groups with respect to the amino hydrogen which favours the $n_N \rightarrow \pi^*_{C–C}$ interactions and at the same time minimizes steric repulsion.

Table 3. Second-order perturbation energies (E_2) in kJ mol^{-1} for charge transfer interactions involving the lone pair at N (n_N) for the four observed conformers of DAA. The atom numbering labels are given in Figures 1 and 4.

Interaction	**I**	**II**	**III**	**IV**
$n_N \rightarrow \pi^*_{C1–C2}$	2.4	2.7	2.4	2.7
$n_N \rightarrow \sigma^*_{C2–C3}$	3.0	7.8	3.0	7.9
$n_N \rightarrow \sigma^*_{C4–C5}$	3.0	3.2	3.5	3.8
$n_N \rightarrow \pi^*_{C5–C6}$	2.4	2.6	–	–
$n_N \rightarrow \sigma^*_{C3–H}$	31.0	2.6	31.3	2.6
$n_N \rightarrow \sigma^*_{C3–H'}$	8.5	31.0	8.7	31.4
$n_N \rightarrow \sigma^*_{C4–H}$	31.0	30.7	31.5	31.3
$n_N \rightarrow \sigma^*_{C4–H'}$	8.5	8.0	8.1	7.6

Conclusions

The conformational landscape of DAA was characterized for the first time using rotational spectroscopy and quantum chemical calculations. Transitions of four conformers were unequivocally identified in the rotational spectrum and their observation allowed for accurate determination of their rotational, quartic centrifugal distortion and ^{14}N quadrupole coupling constants. The theoretical methods employed here identify these four species as energetically very low-lying and the relative abundances from B3LYP-D3(BJ)/aug-cc-pVTZ and single point CCSD(T)/aug-cc-pVTZ//MP2 methods match the trend in experimental intensities. The relative energies from CCSD(T)/ANO0 and MP2/aug-cc-pVTZ calculations offer a slightly different energy ordering for this nearly isoenergetic set of low energy conformers. This highlights the theoretical challenges in quantitatively describing the rich and highly competitive conformational landscape of organic molecules such as DAA and the importance of experimental results to confirm the reliability of quantum chemical methods. Comparing the different geometries of the preferred conformers of DAA, AMA and DADS enhances our understanding of the very complex interactions that govern the physical and chemical properties of allylic compounds. The observed conformational preferences are governed by an interplay of subtle attractive (intramolecular and hyperconjugative) and repulsive effects as supported by NCI and NBO analyses.

Supplementary Material

See supplementary material for pictorial representations and Cartesian coordinates for the 17 low-lying conformers of DAA; list of assigned transitions for conformers I, II, III and IV; predicted spectroscopic parameters at the B3LYP-D3(BJ)/aug-cc-pVTZ and CCSD(T)/ANO0 levels of theory and orbital overlap representations from electronic structure calculations of conformers I, II, III and IV.

Acknowledgements

This research is funded by the Natural Sciences and Engineering Research Council of Canada (NSERC) through the Discovery Grants program. We acknowledge the University of Manitoba for its research computing facility (GREX) and for providing financial support to W.G.D.P.S. through a University of Manitoba Graduate Fellowship. G.D. and S.P. are also thankful to the VP Research Office for funding in the form of Undergraduate Research Awards. The work in Cologne has been supported through the collaborative research center DFG SFB 956 (project ID 184018867, sub-project B3) and by the “Cologne Center for THz Spectroscopy” (grant SCHL 341/15-1). We also acknowledge the Regional Computing Center of the Universität zu Köln for providing computing time on the DFG funded high-performance computing system CHEOPS.

Data Availability Statement

The data that supports the findings of this study are available within the article and its supplementary material.

References

[1] D.H. Barton, Experientia **50**, 390 (1994).

[2] C. Puzzarini and V. Barone, Phys. Chem. Chem. Phys. **22**, 6507 (2020).

[3] M. Melosso, A. Melli, L. Spada, Y. Zheng, J. Chen, M. Li, T. Lu, G. Feng, Q. Gou, L. Dore, V. Barone, and C. Puzzarini, J. Phys. Chem. A **124**, 1372 (2020).

[4] A. Belloche, K.M. Menten, C. Comito, H.S.P. Müller, P. Schilke, J. Ott, S. Thorwirth, and C. Hieret, Astron. Astrophys. **482**, 179 (2008).

[5] N. Kaifu, M. Morimoto, K. Nagane, K. Akabane, T. Iguchi, and K. Takagi, Astrophys. J. **191**, L135 (1974).

[6] N. Fourikis, K. Takagi, and M. Morimoto, Astrophys. J. **191**, L139 (1974).

[7] B.A. McGuire, Astrophys. J. Suppl. Ser. **239**, 17 (2018).

[8] W.G.D.P. Silva, T. Poonia, and J. Wijngaarden, ChemPhysChem **21**, 2515 (2020).

[9] N. Marcelino, J. Cernicharo, M. Agúndez, E. Roueff, M. Gerin, J. Martín-Pintado, R. Mauersberger, and C. Thum, Astrophys. J. **665**, L127 (2007).

[10] M.W. Godfrey, P. D.; Brown, R. D.; Robinson, B. J.; Sinclair, Astrophys. Lett. **13**, 119 (1973).

[11] R.D. Brown, P.D. Godfrey, and D.A. Winkler, Chem. Phys. **59**, 243 (1981).

[12] F. Weinhold, C.R. Landis, and E.D. Glendening, Int. Rev. Phys. Chem. **35**, 399 (2016).

[13] E.R. Johnson, S. Keinan, P. Mori-Sánchez, J. Contreras-García, A.J. Cohen, and W. Yang, J. Am. Chem. Soc. **132**, 6498 (2010).

[14] L. Evangelisti, G. Sedo, and J. van Wijngaarden, J. Phys. Chem. A **115**, 685 (2011).

[15] G. Sedo and J. van Wijngaarden, J. Chem. Phys. **131**, 044303 (2009).

[16] A.D. Becke, J. Chem. Phys. **98**, 5648 (1993).

[17] S. Grimme, S. Ehrlich, and L. Goerigk, J. Comput. Chem. **32**, 1456 (2011).

[18] S. Grimme, J. Antony, S. Ehrlich, and H. Krieg, J. Chem. Phys. **132**, 154104 (2010).

[19] C. Møller and M.S. Plesset, Phys. Rev. **46**, 618 (1934).

[20] T.H. Dunning, J. Chem. Phys. **90**, 1007 (1989).

[21] M.J. Frisch, G.W. Trucks, H.B. Schlegel, G.E. Scuseria, M.A. Robb, J.R. Cheeseman, G. Scalmani, V. Barone, G.A. Petersson, H. Nakatsuji, X. Li, M. Caricato, A.V. Marenich, J. Bloino, B.G. Janesko, R. Gomperts, B. Mennucci, H.P. Hratchian, J.V. Ortiz, A.F. Izmaylov, J.L. Sonnenberg, D. Williams-Young, F. Ding, F. Lipparini, F. Egidi, J. Goings, B. Peng, A. Petrone, T. Henderson, D. Ranasinghe, V.G. Zakrzewski, J. Gao, N. Rega, G. Zheng, W. Liang, M. Hada, M. Ehara, K. Toyota, R. Fukuda, J. Hasegawa, M. Ishida, T. Nakajima, Y. Honda, O. Kitao, H. Nakai, T. Vreven, K. Throssell, J.A. Montgomery, Jr., J.E. Peralta, F. Ogliaro, M.J. Bearpark, J.J. Heyd, E.N. Brothers, K.N. Kudin, V.N. Staroverov, T.A. Keith, R. Kobayashi, J. Normand, K. Raghavachari, A.P. Rendell, J.C. Burant, S.S. Iyengar, J. Tomasi, M. Cossi, J.M. Millam, M. Klene, C. Adamo, R. Cammi,

J.W. Ochterski, R.L. Martin, K. Morokuma, O. Farkas, J.B. Foresman, and D.J. Fox, Gaussian 16, Revision C.01, Gaussian, Inc., Wallingford, CT, 2016.

[22] K. Raghavachari, G.W. Trucks, J.A. Pople, and M. Head-Gordon, Chem. Phys. Lett. **157**, 479 (1989).

[23] J. Almlöf and P.R. Taylor, J. Chem. Phys. **86**, 4070 (1987).

[24] D.A. Matthews, L. Cheng, M.E. Harding, F. Lipparini, S. Stopkowicz, T.-C. Jagau, P.G. Szalay, J. Gauss, and J.F. Stanton, J. Chem. Phys. **152**, 214108 (2020).

[25] M.E. Harding, T. Metzroth, J. Gauss, and A.A. Auer, J. Chem. Theory Comput. **4**, 64 (2008).

[26] J. Contreras-García, E.R. Johnson, S. Keinan, R. Chaudret, J.-P. Piquemal, D.N. Beratan, and W. Yang, J. Chem. Theory Comput. **7**, 625 (2011).

[27] E.D. Glendening, J.K. Badenhoop, A.E. Reed, J.E. Carpenter, J.A. Bohmann, C.M. Morales, P. Karafiloglou, C.R. Landis, and F. Weinhold, NBO 7.0, Theoretical Chemistry Institute, University of Wisconsin, Madison, WI, 2018.

[28] Z. Kisiel, PROSPE - *Programs for rotational spectroscopy*, http://www.ifpan.edu.pl/~kisiel/prospe.htm.

[29] J.K.G. Watson, *in Vibrational Spectra and Structure*, edited by J.R. Durig (Elsevier, New York, 1977), Vol. 6, pp. 1–89.

[30] P.D. Godfrey, R.D. Brown, and F.M. Rodgers, J. Mol. Struct. **376**, 65 (1996).

[31] P.D. Godfrey and R.D. Brown, J. Am. Chem. Soc. **120**, 10724 (1998).

[32] R.S. Ruoff, T.D. Klots, T. Emilsson, and H.S. Gutowsky, J. Chem. Phys. **93**, 3142 (1990).

[33] M.E. Sanz, A. Lesarri, M.I. Peña, V. Vaquero, V. Cortijo, J.C. López, and J.L. Alonso, J. Am. Chem. Soc. **128**, 3812 (2006).

[34] D. Loru, M.M. Quesada-Moreno, J.R. Avilés-Moreno, N. Jarman, T.R. Huet, J.J. López-González, and M.E. Sanz, ChemPhysChem **18**, 274 (2017).

[35] F. Xie, N.A. Seifert, M. Heger, J. Thomas, W. Jäger, and Y. Xu, Phys. Chem. Chem. Phys. **21**, 15408 (2019).

[36] J. Demaison, N. Vogt, R.T. Saragi, M. Juanes, H.D. Rudolph, and A. Lesarri, Phys. Chem. Chem. Phys. **21**, 19732 (2019).